International Journal of Nanomedicine

Dovepress
open access to scientific and medical research

Open Access Full Text Article

ORIGINAL RESEARCH

Magnetic Stimulation of Gigantocellular Reticular Nucleus with Iron Oxide Nanoparticles Combined Treadmill Training Enhanced Locomotor Recovery by Reorganizing Cortico-Reticulo-Spinal Circuit

Juan Li[1,*], Ting Zhou[1,*], Pei Wang[1,*], Ruian Yin[1], Shengqi Zhang[1], Yile Cao[1], Lijuan Zong[1], Ming Xiao[2], Yongjie Zhang[3], Wentao Liu[4], Lingxiao Deng[5], Fei Huang[6], Jianfei Sun[7,*], Hongxing Wang[1,*]

[1]Department of Rehabilitation Medicine, Zhongda Hospital Southeast University, Nanjing, 210024, People's Republic of China; [2]Jiangsu Key Laboratory of Neurodegeneration, Nanjing Medical University, Nanjing, 211166, People's Republic of China; [3]Department of Human Anatomy, Nanjing Medical University, Nanjing, 211166, People's Republic of China; [4]Department of Pharmacology, Jiangsu Key Laboratory of Neurodegeneration, Nanjing Medical University, Nanjing, 211166, People's Republic of China; [5]Department of Neurological Surgery, Spinal Cord and Brain Injury Research Group, Stark Neurosciences Research Institute, Indianapolis, IN, 46202-2266, USA; [6]Institute of Neurobiology, Binzhou Medical University, Yantai, 264003, People's Republic of China; [7]State Key Laboratory of Bioelectronics, Jiangsu Key Laboratory of Biomaterials and Devices, School of Biological Science and Medical Engineering, Southeast University, Nanjing, 210009, People's Republic of China

*These authors contributed equally to this work

Correspondence: Jianfei Sun, State Key Laboratory of Bioelectronics, Jiangsu Key Laboratory of Biomaterials and Devices, School of Biological Science and Medical Engineering, Southeast University, Nanjing, 210009, People's Republic of China, Email sunzaghi@seu.edu.cn; Hongxing Wang, Department of Rehabilitation Medicine, Southeast University Zhongda Hospital, Nanjing, 210024, People's Republic of China, Email 101012648@seu.edu.cn

Background: Gigantocellular reticular nucleus (GRNs) executes a vital role in locomotor recovery after spinal cord injury. However, due to its unique anatomical location deep within the brainstem, intervening in GRNs for spinal cord injury research is challenging. To address this problem, this study adopted an extracorporeal magnetic stimulation system to observe the effects of selective magnetic stimulation of GRNs with iron oxide nanoparticles combined treadmill training on locomotor recovery after spinal cord injury, and explored the possible mechanisms.

Methods: Superparamagnetic iron oxide (SPIO) nanoparticles were stereotactically injected into bilateral GRNs of mice with moderate T10 spinal cord contusion. Eight-week selective magnetic stimulation produced by extracorporeal magnetic stimulation system (MSS) combined with treadmill training was adopted for the animals from one week after surgery. Locomotor function of mice was evaluated by the Basso Mouse Scale, Grid-walking test and Treadscan analysis. Brain MRI, anterograde virus tracer and immunofluorescence staining were applied to observe the tissue compatibility of SPIO in GRNs, trace GRNs' projections and evaluate neurotransmitters' expression in spinal cord respectively. Motor-evoked potentials and H reflex were collected for assessing the integrity of cortical spinal tract and the excitation of motor neurons in anterior horn.

Results: (1) SPIO persisted in GRNs for a minimum of 24 weeks without inducing apoptosis of GRN cells, and degraded slowly over time. (2) MSS-enabled treadmill training dramatically improved locomotor performances of injured mice, and promoted cortico-reticulo-spinal circuit reorganization. (3) MSS-enabled treadmill training took superimposed roles through both activating GRNs to drive more projections of GRNs across lesion site and rebalancing neurotransmitters' expression in anterior horn of lumbar spinal cord.

Conclusion: These results indicate that selective MSS intervention of GRNs potentially serves as an innovative strategy to promote more spared fibers of GRNs across lesion site and rebalance neurotransmitters' expression after spinal cord injury, paving the way for the structural remodeling of neural systems collaborating with exercise training, thus ultimately contributing to the reconstruction of cortico-reticulo-spinal circuit.

Keywords: gigantocellular reticular nucleus, locomotion, magnetic stimulation, spinal cord injury, superparamagnetic iron oxide nanoparticles, treadmill training

Received: 2 April 2024
Accepted: 6 July 2024
Published: 23 July 2024

Graphical Abstract

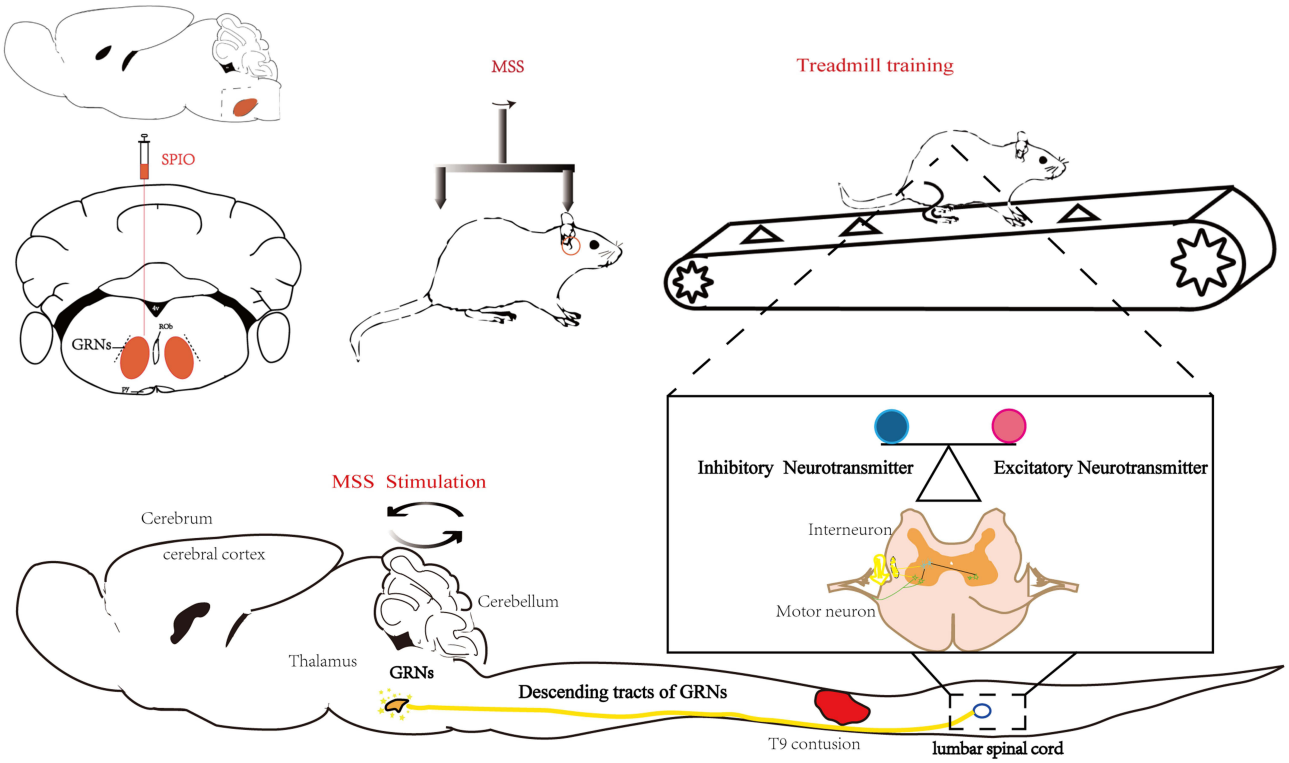

Introduction

Spinal cord injury (SCI) is a life-altering event, characterized by the disruption of descending fibers between the brain and spinal cord, resulting in loss of supraspinal control over the lumbar spinal locomotor center. This often leads to lifelong impairment or paralysis due to the limited capacity of the central nervous system for self-repair and the narrow options for effective treatment.

Most patients experience anatomically incomplete SCI, leaving some spared or surviving fibers detectable by anatomical,[1] imaging[2] and electrophysiological[3] tools. However, approximately half of these patients suffer complete loss of muscle control and sensation below the injury level, indicating that the spared connections are inactive.[4] The gigantocellular reticular nucleus (GRNs) is the origin site of most spared reticulospinal projections following SCI according to evidence from retrograde tracer techniques,[5,6] which relays the output from its upstream target, the mesencephalic locomotor region (MLR), to the spinal cord.[7,8] GRNs were confirmed to target ventral spinal laminae in which rhythm- and pattern-generating interneurons reside, and enough to elicit locomotor behavior upon optogenetic activation.[9] In addition to shaping locomotor patterns and rhythms in freely behaving mice,[10,11] GRNs also play a central role in locomotor recovery after spinal cord contusion in rodents,[6,12] primates and human patients.[13,14] GRNs' projections mediated the volitional modulation from motor cortex to spinal cord Vsx2:Hoxa10 neurons identified by optogenetic single-unit recordings, laying the foundation for volitional locomotion recovery.[15]

Lumbar executive centers that often maintain anatomical integrity can be targeted to induce stepping movement by electrostimulation,[16,17] because of their typically distal location from the lesion site. Nevertheless, surviving fibers alone are unable to elicit volitional movements in severe spinal cord injuries and contribute to limited amelioration in moderate

injuries. The reason why those spared descending fibers cannot improve the locomotion further can be explained by excitatory inhibition of uncontrolled lumbar executive centers due to breakage of descending fibers, and conduction failure of spared fibers.[5,18] Thus, how to activate the dormant GRNs' descending fibers to promote the recovery of motor function after SCI becomes the problem is what we wanted to explore.

The extracorporeal magnetic stimulation system (MSS),[19] a novel neuromodulation technique, consists of targeted delivery of superparamagnetic iron oxide (SPIO) nanoparticles and an extracorporeal magnetic field designed to activate the specific regions containing SPIO nanoparticles. This differs from repetitive transcranial magnetic stimulation (rTMS) therapy, which has demonstrated limited focus and depth of targeted regions.[20] SPIO nanoparticles have shown benign histocompatibility and can be utilized for neuromodulation.[21] Convincing evidence has been provided to support the effectiveness of MSS. For example, depressive-like symptoms were rapidly improved by MSS activating the left prelimbic cortex in depressed mice,[19] and locomotor defects were alleviated by MSS stimulating the striatum in Parkinson's disease rats,[22] even in rats with spinal cord transection.[23]

For most of SCI patients, exercise training, such as weight-supported treadmill training, robot-supported training, and elliptical training,[24] remains the most common and accessible options for triggering and maintaining lumbar spinal cord (LSC) excitability that is required for functional recovery. Treadmill training has been scientifically demonstrated to enhance spinal cord excitability and facilitate the recovery of motor function following SCI in both clinical and animal studies.[25–27] Furthermore, evidence suggests that combining treadmill training with neuromodulation techniques can yield even more favorable outcomes,[28,29] as observed in our groups' previous findings.[30,31]

Since most surviving or spared fibers originate from the GRNs,[5] we hypothesized that stimulating GRNs with MSS could improve the efficiency of the spared fibers and connections within the LSC, enhancing locomotor functional recovery. Moreover, MSS-enabled treadmill training can further amplify the functional capacity of spared fibers, leading to even greater improvements in locomotion. Thus, we confirmed the stability and safety of SPIO nanoparticles in GRNs first. Depending on intervention of MSS-enabled treadmill training, we next investigated the effect of the intervention and possible mechanisms. Results indicated that selective MSS intervention of GRNs promote more spared fibers of GRNs across lesion site and rebalance neurotransmitters' expression after spinal cord injury, which paved the way for the structural remodeling of neural systems collaborating with exercise training, thus ultimately contributing to the reconstruction of cortico-reticulo-spinal circuit.

Materials and Methods

Animals

All experimental procedures were approved by the Animal Ethics Committee of Nanjing Medical University (license No. IACUC-2211044) and were conducted under the committee's guidelines. Experiments were performed on adult female C57BL/6 mice (20–22 g body weight, 8–9 weeks of age) housed at 25 ± 2 °C under a 12 h light/dark cycle. Mice were held five per cage with free access to food and water ad libitum. The entire experiment was divided into two parts, following the principle of using an optimal number of animals (experimental design shown in Figure 1A–C).

Spinal Cord Contusion Injury and Post-Surgical Animal Care

Before surgery, mice were fasted for 12 hours. The procedure of spinal cord contusion injury was performed by Louisville Injury System Apparatus (LISA) impactor (Louisville, KY, 014403), as described previously.[32] Briefly, under aseptic conditions and general anesthesia with isoflurane (5% induction, 1–2% maintenance), spinal cord was exposed at T9-T10 vertebral level, with the spinal column stabilized before laminectomy. Tissue displacements were controlled at 0.5 mm by impact tip monitored by the laser beam, driving by the pressure of the nitrogen tank at 124 kPa. After impact, the spinal cord rapidly developed edema and congestion. Following the muscle-skin suture, the mice were given 1 mL of 0.9% saline subcutaneously, 100 mg/kg ampicillin intraperitoneally to prevent postoperative infection, and subcutaneous injection of carprofen 5 mg/kg to reduce pain. Ampicillin (100 mg/kg) and carprofen (5 mg/kg) were provided for 5 and 3 d after surgery, respectively. Manual urination was performed after surgery at least twice per day until the ability of autonomous micturition recovered.

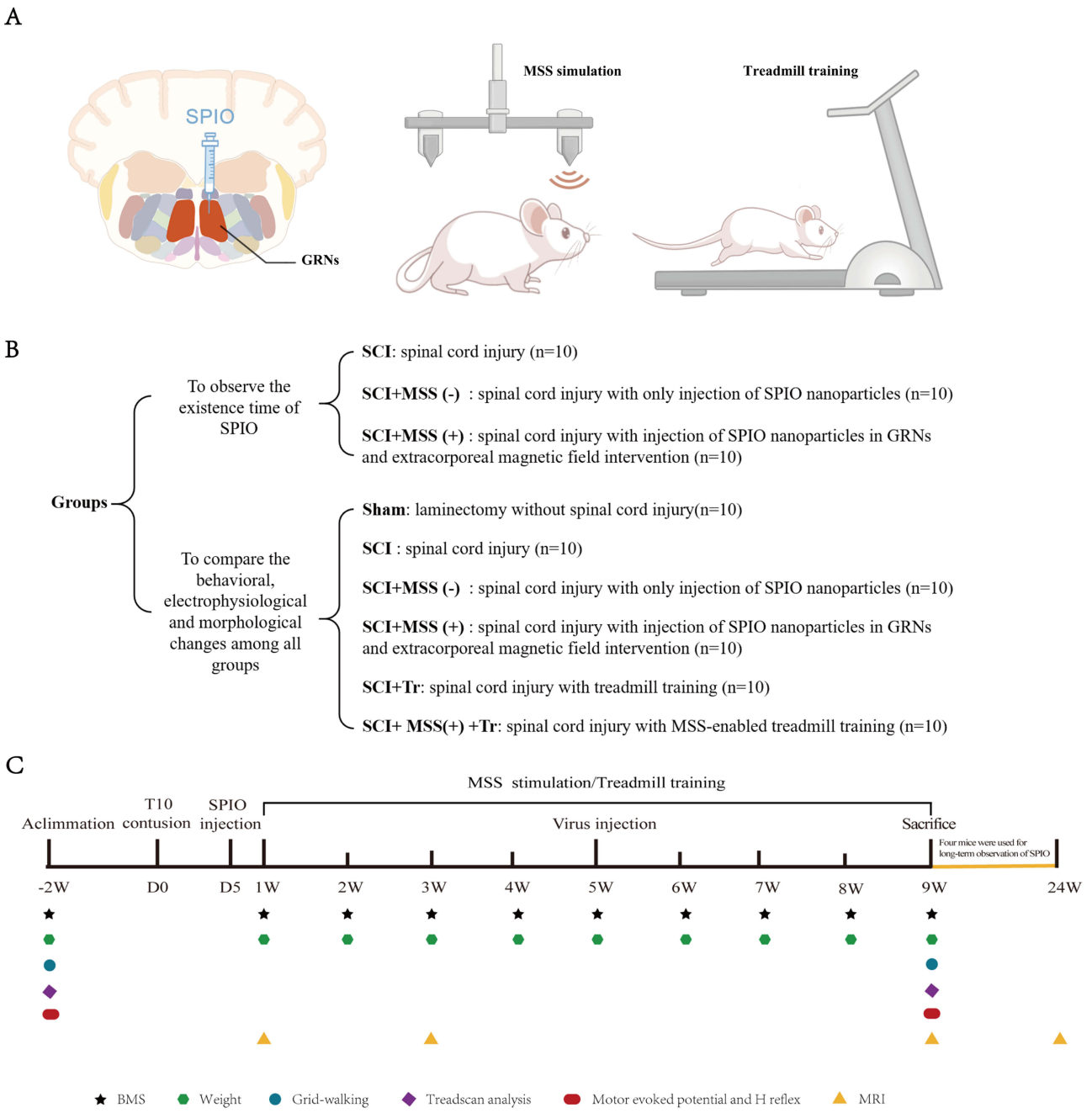

Figure 1 Experimental Design. (**A**) Schematic diagram of the experimental procedure. After injecting SPIO into the GRNs region, mice in SCI+MSS (+) group would be subjected to extracorporeal magnetic field intervention, and mice in SCI+MSS (+) +Tr group would undergo treadmill training immediately after receiving external magnetic field intervention. (**B**) Experimental groups. (**C**) A timeline of the entire experiment, including the time points of different interventions and related evaluations.

Brain Injection

Delivery of SPIO nanoparticles into the GRNs was performed on the fifth day after SCI. The SPIO nanoparticles were polyglucose sorbitol carboxymethylether (PSC)-coated γ-Fe2O3 nanoparticles (trade name: Ferumoxytol), manufactured by Zhengda Tianqing Pharmaceutical Enterprise (China) and approved by the Chinese FDA for clinical use. After successful anesthesia, the mice were immobilized on a stereotaxic apparatus, with exposure of injection site by craniotomy. The injection location of GRNs for mice was anteroposterior (AP): −6.5 mm, mediolateral (ML): ±0.3 mm, dorsoventral (DV): −6.1 mm. 1 μL (2 μg/μL) SPIO nanoparticles were bilaterally injected in GRNs (1 μg per site) using machine-stringed capillary (WPI, 504949, inner diameter=20 μm) with 50 nl/min-controlled by Langer

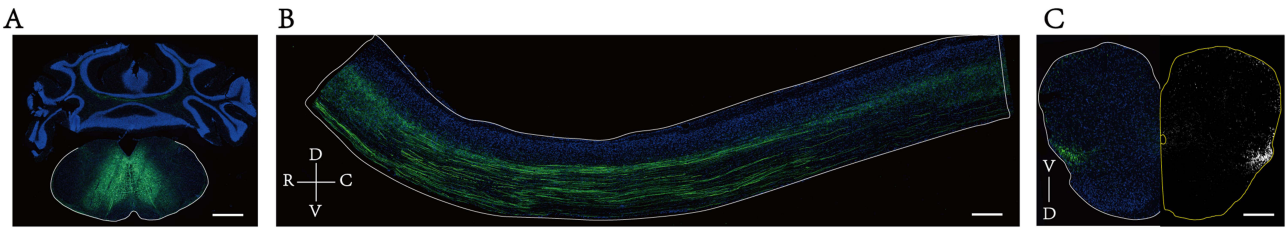

Figure 2 Injection site of GRNs in the brainstem and its projection patterns in the spinal cord. (**A**) rAAV anterograde tracing virus (rAAV-hSyn-EGFP-WPRE-hGH pA) was bilaterally injected at GRNs in the brainstem according to anatomical localization, resulting in neuronal cell bodies expressing green fluorescence at the injection site. (**B**) Projections of GRNs tracing along the sagittal plane of the thoracolumbar spinal cord, as shown by green fluorescence. (**C**) Projections of GRNs distributed in the coronal plane of the lumbar spinal cord, represented by the green fluorescence image on the left side and the grayscale image on the right side. Bar=1000 μm.
Abbreviations: R, rostral. C, caudal; D, dorsal; V, ventral.

microinjection pump (Longer, TJ-2A, China). The capillary was maintained in place for 10 min before slow retraction to prevent reversal of the liquid.

An anterograde virus tracer (rAAV-hSyn-EGFP-WPRE-hGH pA) was bilaterally injected in GRNs at four weeks after SPIO injection, 300 nl per injection site with 30 nl/min (injection site of GRNs and its projection patterns in the spinal cord shown in Figure 2A–C).

Extracorporeal Magnetic Stimulation

Magnetic pulse sequence was generated by the rotation of a pair of tapered magnets (NdFeB permanent magnet, N45, Innuovo, China) symmetrically attached to a motor (IKA RW20 Digital, Germany) using a rigid plastic crossbar. The heads of the experimental mice were placed within the magnetic field. A rotational speed of 600 r/min produced 1200 magnetic pulses at a frequency of 20 Hz, magnetic intervention lasting 20 minutes each time, twice a day and five days per week for eight weeks. The magnetic field intensity was monitored by gauss meter (HT20, Hengtong, China) to maintain the same magnetic intensity every time during MSS intervention.

Treadmill Training

One week after SCI, mice of SCI+MSS (+) +Tr group underwent treadmill training on running platform (Anhui Zhenghua Biological Instrument Equipment Co., LTD) immediately after MSS intervention, 30 min each time, twice a day and five days per week for weight weeks. The running speed started at a minimum of 3 m/min and gradually increased with the improvement of locomotion function, reaching a maximum speed of 8–10 m/min.

Behavioral Tests

Basso Mouse Scale, Grid-walking test and Treadscan analysis were conducted at different time points as (8:30 AM to 11:30 AM) shown on the experimental timeline (Figure 1C). 30 min acclimation and bladder emptying were needed before every evaluation.

Basso Mouse Scale

Motor function was monitored preoperatively and weekly by visual observation in compliance with the Basso Mouse Scale (BMS) as previously described.[33] Briefly, mice were placed on an open-field platform, with free movement. And they were scored independently by two observers blinded to the group allocation of the animals according to ankle mobility, coordination, paw posture, trunk stability, and tail posture. The scale ranges from zero to nine (from complete flaccid paraplegia to normalization, higher scores indicating greater functional recovery).

Grid Walking Test

Grid Walking Test was performed before SCI and at the endpoint of experiment on a horizontal grid, 58 cm length × 20 cm width, 35 cm height, and 1.2 cm×1.2 cm per cell for mice free walking, as previously described.[34] Three-day adaptive training was needed for the mice to walk on a horizontal grid. Foot drops of 30 steps in both sides on the grid were recorded three times.

Treadscan Analysis

The treadscan analysis device includes an enclosed walkway, a cold light high-speed camera (640 × 480, 120 fps, 1/4 CCD), data collection and processing software (Beijing Zhongshi Dichuang Technology Development Co. LTD, ZS-BT /S, China). With footprint light refraction technology, green fluorescent footprints can be captured by the camera. Gait parameters, including footprint area, duration, walking speed, stride length and foot pressure were collected and analyzed by the treadscan system at baseline and the endpoint of experiment.[35]

Observation of SPIO Nanoparticles by MRI Scan

Mice were anesthetized with isoflurane (5% induction, 1–2% maintenance) and immobilized in a stereotaxic frame with a respiration sensor attached to the abdomen. The T2-weighted recordings were performed by 7.0 T magnet (Bruker BioSpec Horizontal 7.0 T). The imaging parameters were as follows: matrix (MTX): 256 × 256, field-of-view (FOV): 2.30/2.00 cm, slice thickness (SI): 0.7 mm, number of contiguous coronal slices: 18, echo time (TE): 42.4 ms and repetition time (TR): 3000 ms. In vivo MRI scans were performed at 2d, 2w, 8w and 24w respectively (n=4) after microinjection of SPIO in the GRNs.

Motor-Evoked Potentials

Motor-evoked potentials (MEPs) of gastrocnemius muscle of different groups were elicited using the previous method[36] at the following time points: pre-operative, 1w and 9w post-operation respectively. Briefly, the mice were anesthetized and placed on a 37°C blanket. The stimulation needle electrodes were inserted subcutaneously over the skull. The cathode of the electrode was placed in direct contact with the bone along the midpoint of an imaginary line connecting the two ears, while the anode was positioned at the base of the nose. The recorded electrode was inserted into the gastrocnemius muscle, with the ground electrode placed on the base of the tail. A single pulse of electrical stimulation (10 mA, 0.1 ms, 1 Hz) to excite the brain was delivered via electromyography stimulator (Haishen Medical Electronic Instrument Co., NDI-097, Shanghai, China). The latency and peak-to-peak amplitude of the trace were recorded and analyzed.

H Reflex

H reflex was induced according to the method of our previous study[31] at pre-operation and 9w post-operation, via electromyography stimulator (Haishen Medical Electronic Instrument Co., NDI-097, Shanghai, China). Stimulus intensity was gradually increased until maximal and stable H-responses were elicited. The latency and amplitude of H waves were recorded at the following stimulation frequencies of 0.1, 0.5, 1 and 5 Hz respectively.

Tissue Processing

Animals were sacrificed at the endpoint of experiment. After deep anesthesia, cardiac perfusion was performed using a perfusion pump (Cole-Parmer, USA) with 0.9% sodium chloride solution followed by perfusion with 4% PFA. Brain and spinal cord tissues were collected and post-fixed in 4% PFA at 4°C overnight, then dehydrated in 20% and 30% sucrose. Tissues were embedded with OCT and cut into 25 μm slices by a Leica cryostat (Wetzlar, Germany). The slices were stained for immunochemical test or frozen at −20°C in PBS glycerin for other tests.

TUNEL Assay

Following the manufacturer's instructions, terminal deoxynucleotidyl transferase-mediated deoxyuridine triphosphate nick end-labeling (TUNEL) with BrightRed Apoptosis Detection Kit (Vazyme, A113-01) was performed for cell apoptosis. Briefly, following the fixation and sectioning of brain tissue, sections were permeabilized and incubated with the TUNEL reaction mixture in a humidified chamber at 37°C for 60 min, and then the tissues were counterstained with DAPI for 5 min. Two images of each slice were taken at 10 X magnification (six mice per group). The total number of apoptotic nuclei was counted using ImageJ software and analyzed by GraphPad Prism 8.0.

Immunochemistry

Immunostainings of c-Fos were performed on brain slices, vglut2, GAD67 and vesicular GABA transporter on spinal cord slices according to the routine procedure of immunochemistry. Primary antibodies included: rabbit anti-c-Fos (Abcam, ab222699, 1: 200), mouse anti-Neun (Sigma-Aldrich, MAB377, 1:400), rabbit anti-vglut2 (Invitrogen, PA5-119621, 1:500), mouse anti-GAD67 (Sigma-Aldrich, MAB5406, 1:500), goat anti-choline acetyl transferase (CHAT) (Sigma-Aldrich, AB144P, 1:200), rabbit anti-vesicular GABA transporter (vGAT) (Merck Millipore, AB5062P, 1:1000). The corresponding fluorescent-conjugated secondary antibodies were applied for 2 h, and the nuclei were stained with Hoechst (Beyotime, 33342, 1:1000).

Quantification of GRNs' Projections

With lesion site as the center, a 10 mm spinal cord specimen was prepared for sagittal sectioning on a Leica cryostat. Starting from the central canal of the spinal cord, sections were taken from both sides every 6 sections for staining analysis. A total of twenty-four sections were selected from six mice in each group. Defining the lesion site as the zero point (0 μm), the fluorescence integrated density (IntDen) of the tracer GFP was then quantified at 700 μm (rostral end of the lesion), 0 μm, −700 μm, and −1400 μm (caudal end of the lesion).

Lumbosacral enlargement was coronally sectioned to analyze the distribution of GRNs' projections in LSC. One section was selected from every 10 sections for staining analysis. Three sections of each animal were chosen and a total of eighteen sections were collected from six mice of each group.

Statistical Analysis

All data involved in this experiment are represented by mean ± SD. GraphPad Prism 8.0 software was used for data analysis. Two-way repeated-measures analysis of variance (ANOVA) was employed to examine data of the BMS score, latency of H reflex and Hmax/Mmax ratio. One-way ANOVA was performed to assess data of the remaining behavioral tests and immunochemistry. A non-parametric test (Kruskal–Wallis test) was used and Dunn's Test for further multiple comparisons if statistical data did not conform to a normal distribution and in case of homogeneity of variance. $P < 0.05$ indicated that the difference was statistically significant.

Results

Stability and Safety of SPIO Nanoparticles in GRNs

Considering that magnetic effects are related to iron content, the doses and concentrations selected according to the results of previous studies were demonstrated to be safe and effective.[19,22,37] According to the experimental timeline (shown in Figure 1C), after delivery of SPIO nanoparticles to GRNs, the distribution and existence was dynamically monitored by MRI (Figure 3A). Images of MRI showed that SPIO nanoparticles were stable and degraded slowly, existing at least 24 weeks. Furthermore, there was no obvious difference in the stability of SPIO nanoparticles between SCI+MSS (-) and SCI+MSS (+) group. It meant that MSS intervention did not interfere in the stability of SPIO nanoparticles in the brain. Next, we used TUNEL assay to evaluate in vivo safety of SPIO. Similar to previous studies,[19] there was no significant difference in percentages (%) of TUNEL-positive cells in GRNs between groups (Figure 3B and Supplementary Figure 1A). SPIO nanoparticles had no short- or long-term influences on the survival quality of mice because there were no significant changes in weight loss at one week after injection and at 9 weeks after SCI between groups (Supplementary Figure 1B). Overall, SPIO nanoparticles delivered to the GRNs were relatively stable and exhibited almost no toxicity on local neurons.

Enhanced Locomotor Recovery with MSS-Enabled Treadmill Training

Anterograde tracing virus was injected into bilateral GRNs of intact mice to observe the trajectory and distribution of descending fibers in LSC (Figure 2A–C). Consistent with previous reports,[38] GRNs' descending fibers traveled along the ventral and lateral funiculus in spinal cord, and their terminals were mainly distributed in the intermediate and ventral zones of LSC, which received command of movements from supraspinal control and implemented voluntary locomotion.

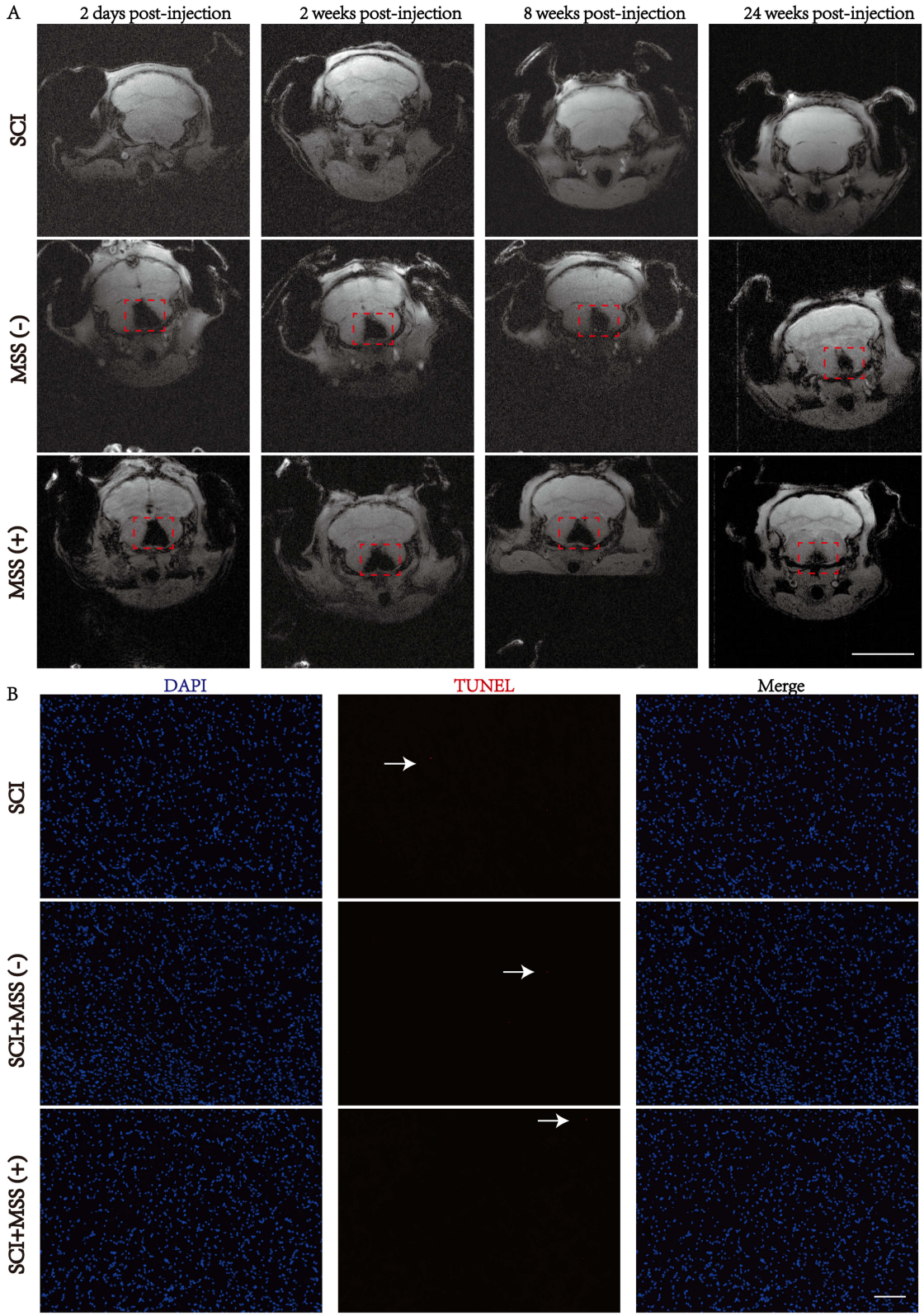

Figure 3 Stability and safety of SPIO nanoparticles in GRNs. (**A**) In vivo coronal MRI images of SPIO nanoparticles in GRNs. After injecting SPIO into the GRNs region, mice in SCI, SCI+MSS (-) and SCI+MSS (+) groups were evaluated by MRI in vivo at 2 days, 2 weeks, 8 weeks and 24 weeks post-injection. The red dashed box indicates the region of SPIO injection. n=4; Bar=5mm. (**B**) TUNEL staining of GRNs region. Representative images of TUNEL-positive nuclei (red color) (x10 magnification) were shown at SCI, SCI+MSS (-) and SCI+MSS (+) groups after 8 weeks of SPIO injection. The white arrows indicate TUNEL-positive cells. Bar=100 μm; n=6.
Abbreviations: MRI, Magnetic resonance imaging; SPIO, superparamagnetic iron oxide; GRNs, gigantocellular reticular nucleus.

To explore the effects of different interventions on recovery of motor function after SCI, mice were divided into Sham, SCI, SCI+MSS (-), SCI+MSS (+), SCI+Tr and SCI+ MSS (+) +Tr group (Figure 1B). Mice exhibited flaccid leg paralysis immediately after the injury and some spontaneous motor function recovery occurred at 1 week after injury, characterized by some ankle movements without weight support. All injured mice displayed varying degrees of improvement in locomotion function at nine weeks after SCI, in comparison to one-week post-SCI (Figure 4A). There were no obvious differences in BMS scores between SCI group and SCI+MSS (-) group at each time point, with scores tending to plateau around 7 weeks. The delayed effects of MSS intervention on motor function recovery were observed, with visible improvements appearing at four- or five-weeks post-injury, and statistically significant improvements were observed at six weeks post-injury in the SCI+MSS (+) group, compared with SCI group. Treadmill training expedited improvement in locomotor performance evidenced by statistically significant increases in BMS score after three weeks' training, compared with SCI group ($P<0.05$). Although treadmill training alone seemed to be superior to single MSS intervention, there were no statistically significant differences in BMS scores found between two interventions. However, mice in the SCI+ MSS (+) +Tr group exhibited the better locomotor improvement among the groups with consistent and coordinated plantar stepping. The grid walk test was used to assess limb movements related to sensorimotor functions, such as precise walking, coordination, and accurate placement of paws.[39] There were no significant differences in foot drops between the SCI and SCI+MSS (-) groups (Figure 4B). Both MSS intervention and treadmill training individually showed a positive effect on alleviating foot drops, compared to SCI group. Excitingly, the mice in SCI+ MSS (+) +Tr group showed the lowest foot drops among those groups except Sham group. Meanwhile, we conducted an unbiased Treadscan analysis to measure locomotion according to more detailed parameters, including footprint area, footprint strength and swing speed (Figure 4C–E). Compared with SCI group, regarding occasional plantar stepping, the footprint area, strength and swing speed improved significantly both in SCI+MSS (+) and SCI+Tr group which displayed consistent plantar stepping. But there were no statistically significant differences observed in those parameters between treadmill training and MSS intervention groups. Compared with SCI+MSS (+) and SCI+Tr group, the mice in SCI+ MSS (+) +Tr group showed the greater performance in swing speed, footprint area and footprint strength (Figure 4F and G).

Overall, these findings indicated that both MSS intervention and treadmill training individually could make slight improvements in motor function. However, MSS-enabled treadmill training facilitated more greater improvements in locomotor functional recovery.

MSS-Enabled Treadmill Training Reorganized Cortico-Reticulo-Spinal Circuit and Modulated Motor Neuron Excitability

Given that GRNs relayed the commands from the MLR[40] and motor cortex[5] to LSC center, the excellent locomotor recovery observed in the SCI+ MSS (+) +Tr group was presumed to be contributed from cortico–reticulo–spinal circuit reorganization. We evaluated MEPs which reflected the integrity of motor pathways.[41] Consistent elicitation of MEPs was observed before SCI, whereas MEPs were absent one week after injury among groups except Sham group (Supplementary Figure 1C). At 9 weeks post-injury, MEPs failed to be elicited in both SCI and SCI+MSS (-) groups, even in SCI+MSS (+) and SCI+Tr groups despite some locomotor improvement (Figure 5A). Amazingly, SCI+MSS (+) +Tr group did successfully induce MEPs, albeit with smaller amplitude (Sham vs SCI+MSS (+) +Tr, 9.55± 1.0928 mV vs 0.70959± 0.57379 mV) and longer latency periods (4.305±0.188 ms vs 23.085±1.60 ms) compared to intact mice. The percentage of MEPs evoked in SCI+ MSS (+) +Tr group was 60% (6 out of 10 mice) (Figure 5B).

H reflex is commonly used to examine motor neuron excitability and spasticity in both clinical and animal studies. All groups showed rate-dependent depression of Hmax/Mmax ratio, with stimulation frequency of 0.1, 0.5, 1 and 5 Hz (Figure 5C). The ratio in SCI group was higher at same stimulation frequency than other groups. A significant reduction in Hmax/Mmax ratio was observed both in the SCI+ MSS (+) +Tr group and SCI+Tr group compared to SCI group, especially at stimulation frequencies of 0.1 Hz ($P<0.0001$). Hmax/Mmax ratio of SCI+ MSS (+) group also exhibited non-statistical decreases compared to SCI group at every stimulation frequency. It was worth noting that the latency of H reflex became prolonged with stimulation frequency increased between groups (Figure 5D). In Sham group, H-waves

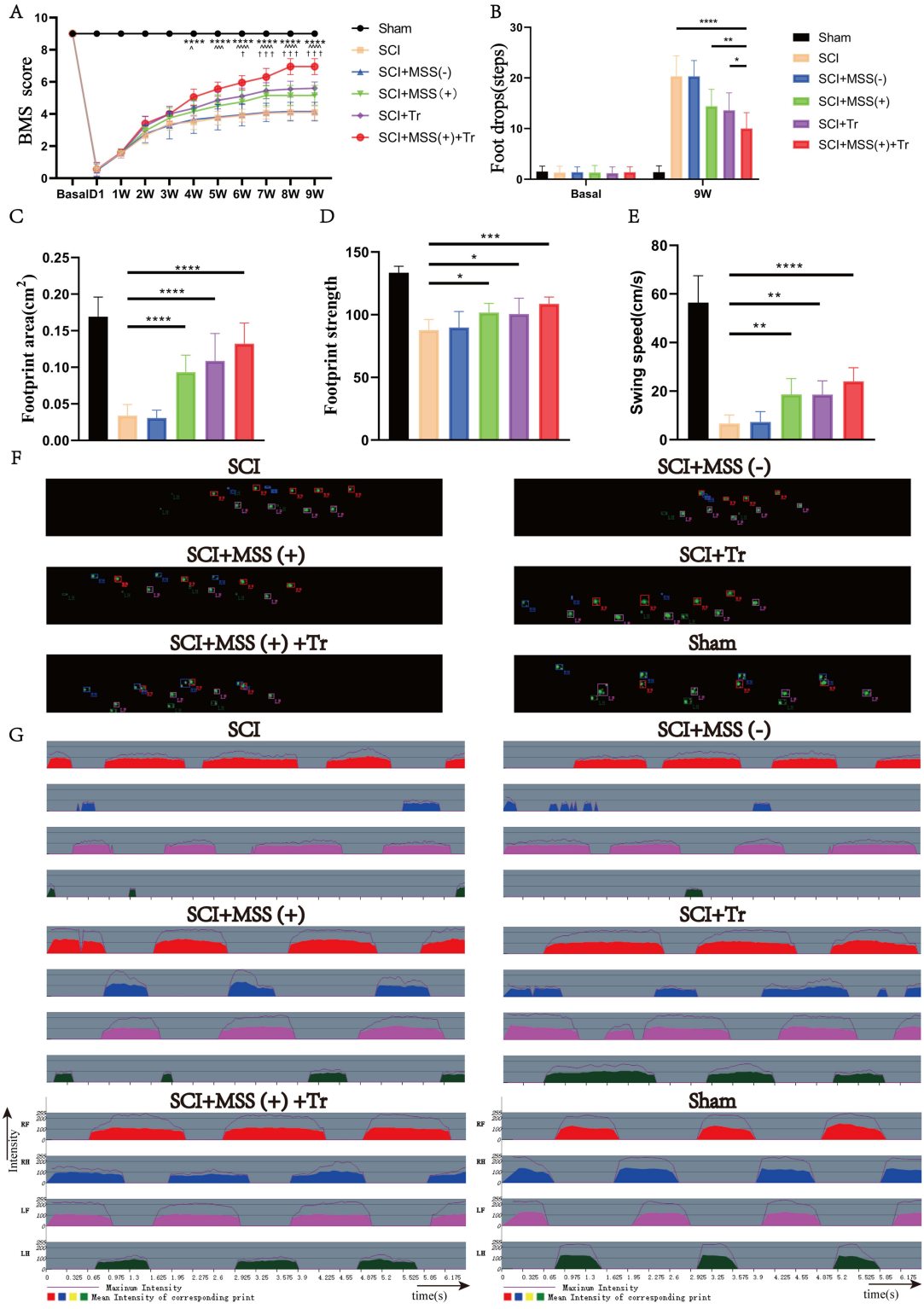

Figure 4 Locomotor recovery was enhanced prominently by MSS-enabled treadmill training. (**A**) BMS scores were analyzed (n = 10 mice per group at each time point). †Represented a comparison between the SCI group and SCI+MSS (+) group (†P < 0.05; †††P < 0.001); ^represented a comparison between the SCI group and SCI+Tr group (^P < 0.05; ^^^P < 0.001); *represented a comparison between the SCI group and SCI+ MSS (+) +Tr group (****P < 0.0001). Two-way repeated-measures ANOVA with Fisher's LSD. (**B**) Grid walking test was performed in the same six groups (n = 10 mice per group at each time point) by two-way ANOVA with Tukey's test. P < 0.05; **P < 0.01, ****P < 0.0001. (**C**–**E**) The footprint area, footprint strength and swing speed of the hindlimbs respectively were evaluated in the same six groups (n = 10 mice per group at each time point) by Dunn's Test for multiple comparisons. *P < 0.05; **P < 0.01, ***P < 0.001, ****P < 0.0001. (**F**) Representative images of footprint area were shown in each group exported by Treadscan device. (**G**) Representative images of footprint strength were shown in each group exported by Treadscan device. Data are presented as means ± SD.

Abbreviations: LF, left foot; LH, left hand; RF, right foot; RH, right hand.

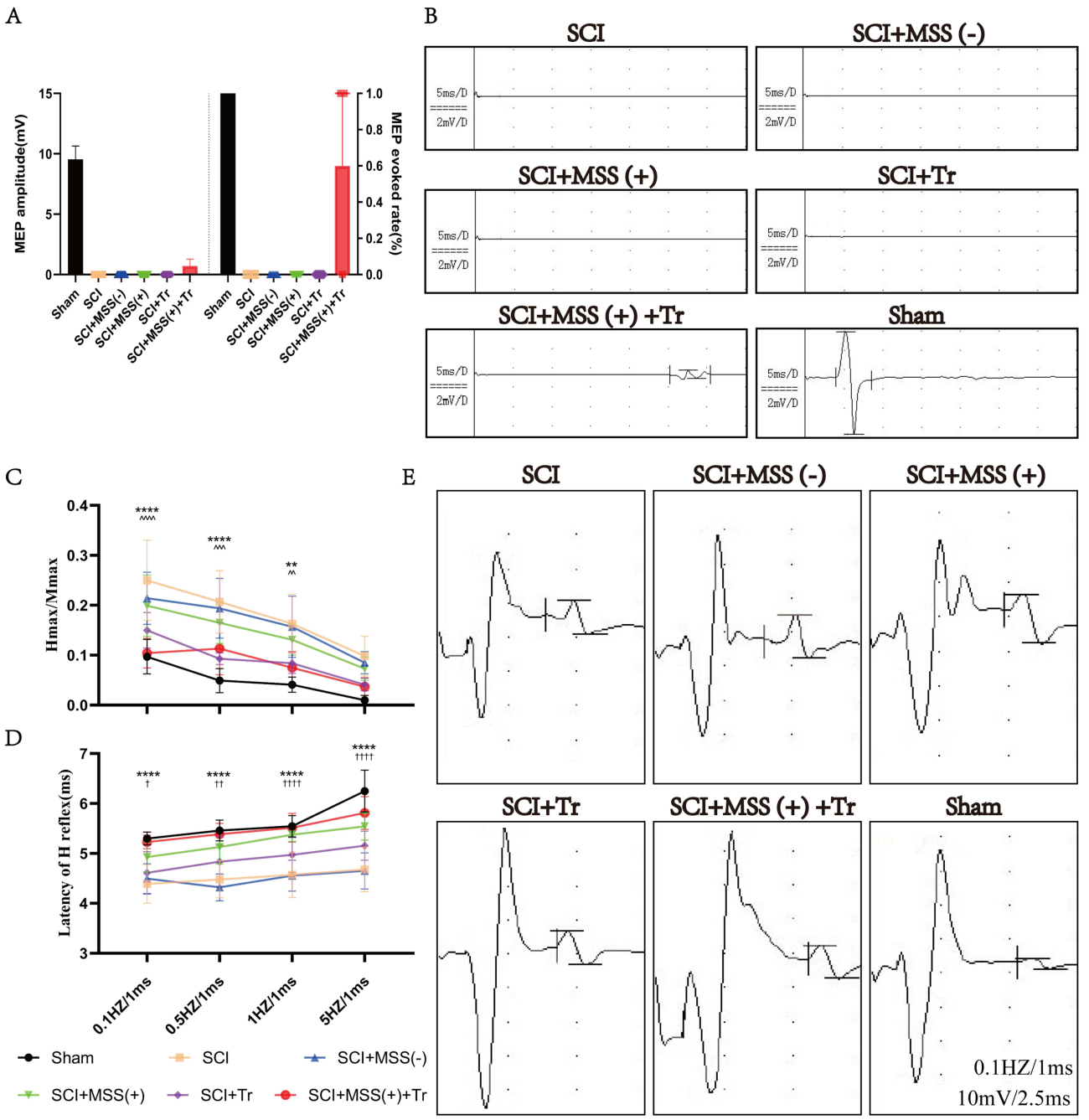

Figure 5 Motor neuron excitability was modulated by MSS and cortico-reticulo-spinal circuit was reorganized by MSS-enabled treadmill training. (**A**) Cortico–reticulo–spinal circuit reorganization was reflected by evocation of MEP only in mice of SCI+MSS (+) +Tr group after SCI could be successfully evoked. The amplitude of MEP in Sham group was 9.55 ± 1.0928 mV, and in SCI+MSS (+) +Tr group, it was 0.70959 ± 0.57379 mV. It was shown in left side. The evoked rate of MEP, shown at right side, was 100% in Sham group (10 out of 10), and 60% in SCI+MSS (+) +Tr group (6 out of 10). (**B**) Representative images of MEP in each group. Except for the Sham group and the SCI +MSS (+) +Tr group, none of the other four groups were able to induce MEP after SCI. Although the MEP amplitude and latency were lower and longer, respectively, in the SCI+MSS (+) +Tr group compared to the Sham group, this represents a reorganization of the cortico-reticulo-spinal circuit. (**C** and **D**) Motor neuron excitability was reflected by H reflex. Statistical analysis of the Hmax/Mmax and latency of H reflex in different groups (n = 10) at 0.1 Hz, 0.5 Hz, 1 Hz and 5 Hz was shown in (**C** and **D**), respectively. †Represented a comparison between the SCI group and SCI+MSS (+) group (†P < 0.05; ††P < 0.01; ††††P < 0.0001); ^represented a comparison between the SCI group and SCI+Tr group (^^P < 0.01; ^^^P < 0.001; ^^^^P < 0.0001); *represented a comparison between the SCI group and SCI+ MSS (+) +Tr group (**P < 0.01; ****P < 0.0001). Two-way repeated-measures ANOVA with Fisher's LSD. (**E**) Representative electromyogram signal of eliciting H reflex in different groups at 0.1 Hz.

were less observable with significantly delayed latency at 5 Hz stimulation, whereas it still appeared in SCI group. Interestingly, MSS intervention distinctly increased the latency of H-waves at each stimulation frequency compared to SCI group. However, treadmill training alone did not significantly prolong the latency of the H reflex. In SCI+ MSS (+)

+Tr group, the latency of H reflex was delayed with no significant difference compared with Sham group (representative H reflex at 0.1 Hz shown in Figure 5E).

In brief, these findings indicated that MSS-enabled treadmill training may reduce excitability of motor neurons and alleviate spasticity of SCI animals by decreased Hmax/Mmax ratio and delayed latency of H reflex, which supported reorganization of cortico-reticulo-spinal circuit and reintegration of motor pathway reflected by successful eliciting of MEPs.

MSS Intervention Fired More GRNs' Projections Across the Lesion Site

c-Fos protein, as a marker of neuronal activity,[42] was examined to verify the activation of GRNs. The results showed that MSS intervention induced more c-Fos expression in neurons located within the GRNs compared with Sham, SCI, SCI +MSS (-) and SCI+Tr groups (Figure 6A and D). It meant that local neurons in GRN could produce biological responses to MSS intervention.

Further, we investigated whether MSS intervention could change GRNs' projections at morphological level. At four weeks after MSS intervention, anterograde virus tracer (rAAV-hSyn-EGFP-WPRE-hGH pA) was injected into GRNs to trace the GRNs' projections into the spinal cord (Figure 2A–C). To quantify the projections of GRNs above and below the lesion site, four sites were taken in sagittal sections referring to the center of lesion site, 700 μm above center, 0 μm (center), and −700 μm, −1400 μm below center respectively (Figure 6B). Compared with Sham group, fluorescent images showed spinal cord contusion resulted in a significant loss of GRNs' projections below the injury site. However, MSS intervention drove more GRNs' fibers across the injury site, compared to SCI and SCI+MSS (-) groups in the sagittal sections of spinal cord. Treadmill training also drove some fibers through the lesion site compared to SCI group. Except for the Sham group, SCI+MSS (+) +Tr group presented larger number of GRN projections at 700 μm and 0 μm than other groups (Figure 6E). According to the coronal section of LSC, GRNs' projections were distributed into the ventral and ventrolateral columns, with high-density projections in the anterior horn enriched around motor neurons (Figure 6C). Similar to the trend in sagittal sections, the SCI+MSS (+) group showed a distinctly higher distribution of GRNs' fibers in the coronal plane of the spinal cord, compared to SCI and SCI+MSS (-) groups (Figure 6F). Compared with SCI+MSS (+) and SCI+Tr groups, SCI+MSS (+) +Tr group owned the largest distribution of GRNs' projections on the coronal plane.

MSS Intervention Rebalancing Neurotransmitters' Expression at Spinal Anterior Horn

Considering that modulating expression of neurotransmitters at spinal anterior horn was found to be critical for improving motor output and training outcomes after SCI,[43,44] expression of excitatory and inhibitory neurotransmitters were all examined. Vglut2, a classic maker of excitatory glutamatergic neurotransmitter in LSC, was extremely low at spinal anterior horn in SCI group (Figure 7A). However, both MSS intervention and treadmill training increased the expression of vglut2 in the anterior horn in contrast with SCI group, which was linked to the improvement of spinal cord excitability (Figure 7D). The expression levels of GAD67 and vGAT, the markers of inhibitory neurotransmitters, were found to be upregulated in the spinal anterior horn following SCI (Figure 7B and C), which aligns with previous studies.[45] With MSS intervention, there was a pronounced decrease in GAD67 and vGAT expression at the anterior horn when compared to SCI group (Figure 7E and F). Nevertheless, treadmill training alone had little effect on the expression of GAD67 and vGAT, suggesting a limited regulation of treadmill training on inhibitory neurotransmissions. Notably, SCI+ MSS (+) + Tr group, which showed excellent motor function recovery, exhibited decreased expression of vglut2, GAD67 and vGAT similar to the levels of Sham group (Figure 7A–F). These results implied that remarkable motor function recovery may be due to the rebalancing of the expression of different neurotransmitters to the intact level in anterior horn, which can be achieved by MSS-enabled treadmill training. Then, we investigated the molecular properties of the GRNs' projections. It is currently known that GRNs contain intermingled neuronal subpopulations.[9,46] Since glutamatergic neurons in the GRN region have been extensively studied for their involvement in motor processes and the recovery of motor function after SCI,[10–12] we initially assessed vglut2. Unexpectedly, despite higher expression of vglut2 and more GRNs' projections at LSC in the MSS (+) group, few downward fibers co-labeled with vglut2 (Figure 7A). Just

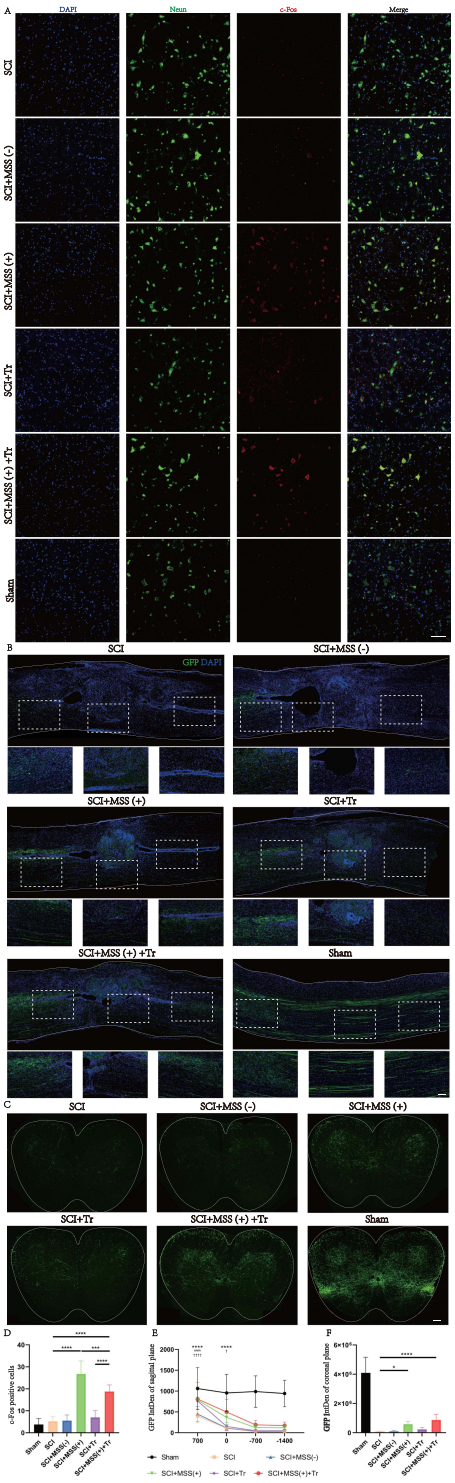

Figure 6 MSS intervention fired more GRNs' projections across the lesion site. (**A**) Representative images of c-Fos positive cells at GRNs region in each group, c-Fos (red) counterstaining with Neuron marker (green), with the size (Unit Converted) 636.396 μm *636.396 μm. Statistical analysis of the numbers of c-Fos positive cells was performed in the same six groups (n = 6 mice per group) by Dunn's Test for multiple comparisons, shown at (**D**) (***P < 0.001; ****P < 0.0001). Bar=100 μm. (**B**) Representative images of GRNs' projections (green) across the lesion site in sagittal sections, as well as higher magnification views at the lesion center, both above and below the center in each group (corresponding to the white dashed box). Quantification of GRNs' projection at four sites in sagittal sections (taking the images with the lesion center as the reference site, one above the center, another two below the center, 700 μm, 0 μm, −700 μm, and −1400 μm respectively) was shown at (**E**). †Represented a comparison between the SCI group and SCI+MSS (+) group (†P < 0.05; ††††P < 0.0001); ^represented a comparison between the SCI group and SCI+Tr group (^^^^P < 0.0001); *represented a comparison between the SCI group and SCI+ MSS (+) +Tr group (****P < 0.0001). Two-way repeated-measures ANOVA with Fisher's LSD. Scale bar: 100 μm, n=6. (**C**) Representative images of GRNs' projections (green) at the lumbar spinal cord according to coronal sections and statistical analysis of GRNs' projections at coronal sections was performed by Dunn's Test for multiple comparisons, shown at (**F**). Scale bar: 100 μm, n=6.

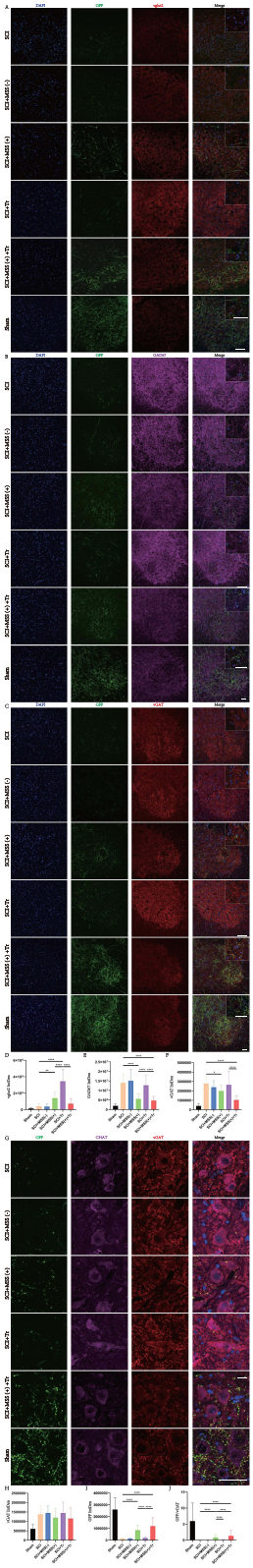

Figure 7 MSS intervention rebalancing neurotransmitters' expression of spinal anterior horn. (**A**–**C**) Representative images of GRNs' projections (GFP) co-stained with vglut2 (red), GAD67 (purple) and vGAT (red) at anterior horn in the lumbar spinal cord, respectively. Higher magnifications depicted in the white box. (**D**–**F**) Statistical analysis of vglut2, GAD67and vGAT expression levels was performed by Dunn's Test for multiple comparisons, respectively (*P < 0.05; **P < 0.01; ****P < 0.0001). Bar=50 μm. n=6. (**D**) Representative images of GRNs' projection (GFP) co-stained for CHAT (purple), vGAT (red) of anterior horn in lumbar spinal cord. (**H**–**J**) Statistical analysis of vGAT, GFP and GFP/vGAT expression levels was performed by Dunn's Test for multiple comparisons, respectively (****P < 0.0001). Bar=50 μm. n=6.

like vglut2, few GAD67 co-labeled with downward GRNs' fibers (Figure 7B). Surprisingly, more than half of GRNs' projections co-labeled with vGAT in SCI+MSS (+) group (Figure 7C).

Next, given that vGAT was primarily distributed in the region motor neurons were located in, we co-stained vGAT with the motor neuron marker CHAT. A notable upregulation of GRNs' projections co-labeled with vGAT on the membrane surface of motor neurons was found in SCI+ MSS (+) group, compared with SCI, SCI+Tr group (Figure 7G). MSS intervention combined with treadmill training resulted in higher GRNs' projections co-labeled with vGAT on the membrane surface of motor neurons, similar to the Sham group. However, there was no difference in overall vGAT expression in the motor neuron region among the groups (Figure 7H). Similar to the distribution of GRNs' projections in the coronal plane at LSC (Figure 6F), the number of GRNs' projections around motor neurons increased after MSS intervention (Figure 7I). GFP/vGAT ratio expression had the same increasing trend (Figure 7J). It is plausible that the increased GRNs' projections co-labeled with vGAT may contribute to the modulation of inhibitory signaling and synaptic transmission on the membrane surface of motor neuron, leading to alleviation of H-reflex and locomotion dysfunction (Figures 4A and 5C).

These converging pieces of evidence indicated that MSS intervention played an important role in promoting locomotion recovery by rebalancing of neurotransmitters' expression at anterior horn of spinal cord. MSS-enabled treadmill training produced superimposed effects on functional recovery after SCI through both reorganization of motor pathway and decreased motor neuron excitability of spinal cord.

Discussion

To date, more research confirms the contribution of spared fibers to locomotion functional recovery following SCI. However, due to the majority of spared fibers being in a dormant state, their full utilization in the recovery of motor function after SCI remains limited. This study used a moderate contusion SCI mice model and activated GRNs by MSS intervention, demonstrating that (1) SPIO persisted in GRNs for a minimum of 24 weeks almost without any apoptosis of GRNs cells, and degraded slowly over time. (2) MSS-enabled treadmill training dramatically improved locomotor performances of SCI mice, and promoted cortico-reticulo-spinal circuit reorganization. (3) MSS-enabled treadmill training took superimposed roles through both activating GRNs to drive more projections of GRNs across lesion site and rebalancing neurotransmitters' expression in anterior horn of LSC.

Contribution of GRNs to Recovery of Spinal Cord Injury

Gene editing and function-ON/Off experiments have revealed that medullary reticulospinal tract (RetST) contributes to the initiation, coordination, and regulation of locomotion.[47,48] Moreover, accumulating evidence has shown that RetST plays an important role in functional locomotion improvement in rodents and primates after SCI, even enhancing voluntary functional recovery in SCI patients.[13,49] GRNs' descending fibers, as a primary component of the RetST, have been identified as a crucial source of the spared reticulospinal projections after SCI. These GRNs play a pivotal role in relaying commands from motor cortex neurons to the LSC evidenced by optogenetic stimulation, modulating the activity of leg muscles during locomotion.[5,15] However, despite the presence of spared reticulospinal projections following SCI, their functionalities can be compromised due to conduction failure. Interestingly, cooling of the lesion site can increase recruitment of these dormant projections and improve behavioral function,[18] indicating that activation of silent fibers is indeed crucial for promoting function.

Strategies to boost conduction of those dormant fibers can be classified into two types. One approach is targeting the area above the lesion to enhance conduction of spared descending fibers, including MLR-DBS,[50,51] cortical electrical stimulation,[52] and TMS.[53] Another one is to act on the area below the lesion, including epidural electrical stimulation and treadmill training. The goals of these approaches are to enhance the functional state of the LSC circuit, allowing it to respond to supraspinal and/or sensory input. Otherwise, the LSC circuitry will remain in inhibited state and then be unable to react effectively to signals transmitted through residual fibers.

Effects of MSS Intervention

The extracorporeal magnetic stimulation system (MSS) utilizes the targeted delivery of SPIO nanoparticles and an extracorporeal magnetic field.[19] This approach elevates magnetic susceptibility of the local tissue, enabling the magnetic effect to act on deep brain structures and enhance the selective magnetic stimulation in targeted region. In this study, we demonstrated that SPIO nanoparticles exhibited relative stability within GRNs, and showed minimal toxicity on local neurons. Additionally, the MSS intervention successfully activated neurons in GRN region with a high level of precision. These findings are consistent with another study,[19] in which MSS rapidly relieved depression-like symptoms in mice by activating the left prelimbic cortex. Similar to this study, MSS intervention promoted the expression of c-Fos in local neurons.

Through MSS intervention to activate GRNs which relay commands between the motor cortex/MLR and LSC, we observed motor function recovery in mice with spinal cord contusion. The majority of supraspinal neuromodulation techniques used to treat SCI are focused on the MLR, an evolutionary conserved motor control region and upstream of GRNs.[54,55] Considering the location of GRNs in the brainstem, the central hub of life-sustaining functions, the manipulation of this region faces technical challenges, such as electrode implantation. Therefore, in order to clarify the effect and mechanism of direct stimulation on spared descending fibers of GRNs, we chose stereotactic targeted delivery of SPIO to GRNs. Due to the fact that GRNs are downstream of the MLR[7] and the clinical feasibility of DBS in the MLR region,[51] subsequent research will explore MSS intervention in MLR for its potential clinical applications. Meanwhile, this study demonstrated the safety and feasibility of SPIO injection to the brainstem, paving the way for future investigation of other brainstem nuclei, particularly in the fields of respiratory and circulatory control.[56]

MSS has also been utilized in Parkinson's disease (PD) and been proven to enhance feeding behavior, gait, and postural stability in PD rats via stimulation of the striatum.[22] Even in rats with spinal cord transection, MSS intervention has been shown to alleviate oxidative stress of local lesion and promote functional recovery.[23] In our results, SCI mice showed poorer motor function with higher Hmax/Mmax ratio and shorter latency of H reflex in lower extremity. As reported in a previous study, overexcitability of motor neurons or hypertonia of muscles could seriously impair the process of motor function recovery. Studies have confirmed that decreased Hmax/Mmax ratio and prolonged latency of reflex is associated with modulated motor neuron excitability and reduced spasticity.[57] Thus, the positive effect of MSS alone in this study was related to the modulation of H-reflex in SCI mice. Spinal cord contusion causes the disruption of descending supraspinal projections including fibers of GRNs, which was also proved by the study of Asboth et al.[5] However, MSS intervention pushes more descending fibers of GRNs across the lesion, similar to how CNF-DBS promotes more CNF's projections to the GRNs.[58] It is emphasized that even though MSS intervention facilitates an increase of GRNs' projections below the site of injury, MEPs representing integrity of CST have not shown any recovery. It is supposed that the lack of exercise intervention, especially lack of task-oriented exercise training resulted in: 1) a majority of the increased projections from GRNs have not formed functional connections with the LSC; 2) the command connectivity between the cortex and GRNs is not tightly established. These speculations were proved by the further results that MEPs were successfully induced after intervention of MSS-enabled treadmill training. So, it meant that MSS and treadmill training produce superimposed effects on functional recovery after SCI.

Unexpectedly, a large portion of GRNs' projections co-labeled with vGAT, which were concentrated in the nerve endings of GABAergic neurons or in glycinergic nerve endings.[59] Considering that spasticity was caused by hyperexcitability of motor neurons[60] and this excessive excitability could be reduced by GABA agonist Baclofen,[61] we hypothesized that modulation of H-reflex is associated with an increased presence of vGAT-GRNs' projections to the motor neuron induced by MSS intervention. Consistent with other studies,[44] SCI resulted in decreased expression of the excitatory neurotransmitter vglut2 and increased expression of the inhibitory neurotransmitter GAD67. However, MSS intervention promoted the expression of vglut2 in spinal anterior horn, reduced the expression of GAD67, and increased the excitability of the spinal cord. This may be associated with a mixed role of excitatory and inhibitory neuronal subpopulation in GRNs.[46] In addition, neurotransmitter phenotypes can switch between excitatory and inhibitory neurons in response to environmental influences, evidenced by the technologies of gene editing, in situ hybridization and immunohistochemistry.[44,62] Further research will be needed to investigate the specific nuclei of GRNs from which the

descending vGAT-projections originate and the predominant muscle (flexor or extensor) that the vGAT-projections are primarily connected to. Pharmacological studies have demonstrated that the regulation of excitation-inhibition (EI) balance in circuits below the injury site is a crucial mechanism that determines the motor capacity of cats and rodents with SCI, irrespective of the age of the injury.[63,64] These findings suggest that the potential mechanism underlying the improvement of motor function by MSS intervention may be related to neurotransmitters' rebalancing at LSC.

Effects of MSS-Enabled Treadmill Training

Exercise training is often prescribed for SCI patients to improve muscle strength and quality, increase spinal cord plasticity, and enhance cardiovascular fitness,[65] though purely exercise-based training has a few limitations in improving voluntary motor function.[66,67] Therefore, in clinical practice, exercise training is mostly combined with task-oriented approaches or neuromodulation techniques, such as robotic-assisted treadmill training incorporating high repetitions of task-oriented practice, TMS and functional electrical stimulation.[68] In the current study, while treadmill training alone and MSS intervention alone showed some degree of motor function recovery, it was not as pronounced as that seen with MSS-enabled treadmill training. Notably, only MSS-enabled treadmill training was accompanied by successful elicitation of MEPs. Although the elicitation of MEPs exhibited lower amplitudes and longer latencies, which may be related to polysynaptic conduction of cortico–reticulo -spinal cord signals rather than monosynaptic transmission via the corticospinal tract. However, the presence of MEPs indicated the integrity of cortical-reticular-spinal signaling pathway. Additionally, treadmill training alone did promote the expression of the excitatory neurotransmitter vglut2 at spinal cord ventral horn, but did not significantly decrease the expression of GAD67 and vGAT. Meanwhile, in the MSS-enabled treadmill training group, significant improvement in motor function was accompanied by a decrease in the expression of excitatory and inhibitory neurotransmitters, giving the impression of reduced "activity" in spinal neurons. This phenomenon was also supported by a clinical trial.[15] Researchers utilized positron emission tomography with 18F-fluorodeoxyglucose uptake to measure the impact of walking before and after the application of EES on metabolic activity of LSC during neurorehabilitation. The results revealed that EES applied during neurorehabilitation led to a reduction of metabolic activity in LSC. To some extent, this phenomenon supported the decrease of c-Fos expression in spinal cord with the recovery of motor function.[69] This reduced neuronal activity in LSC may be associated with activity-dependent selection of specific neuronal subpopulations,[15] reflecting the energy-efficient working modality of the spinal cord under healthy physiological conditions.

Conclusion

These results indicate that intervention of GRNs by MSS may be a novel strategy to drive more spared fibers across the lesion site and rebalance neurotransmitters' expression of anterior horn at lumbar spinal cord after SCI, empowering the structural foundation for exercise training, to achieve reorganization of cortico-reticulo-spinal circuit.

Abbreviations

BMS, Basso Mouse Scale; MSS, magnetic stimulation system; DBS, deep brain stimulation; EES, epidural electrical stimulation; GRNs, gigantocellular reticular nucleus; LSC, lumbar spinal cord; MEPs, Motor-evoked potentials; MLR, mesencephalic locomotor region; SCI, spinal cord injury; SPIOs, superparamagnetic iron oxides; RetST, reticulospinal tract; TUNEL, terminal deoxynucleotidyl transferase-mediated deoxyuridine triphosphate nick end-labeling; vGAT, vesicular GABA transporter.

Ethics Approval

All experimental procedures were approved by the Animal Ethics Committee of Nanjing Medical University (license No. IACUC-2211044).

Consent for Publication

All authors have seen the manuscript, and gave consent to publish all details of this article.

Author Contributions

All authors made a significant contribution to the work reported, whether that is in the conception, study design, execution, acquisition of data, analysis and interpretation, or in all these areas; took part in drafting, revising or critically reviewing the article; gave final approval of the version to be published; have agreed on the journal to which the article has been submitted; and agree to be accountable for all aspects of the work.

Funding

This work was supported by grants from the National Key Research and Development Program of China [Grant No. 2022YFC2009700], Key Medical Program of Jiangsu Commission of Health [Grant No. ZD2022048], Jiangsu Province Capability Improvement Project through Science, Technology and Education, and Jiangsu Provincial Medical Key Discipline Cultivation Unit [JSDW202202], National Natural Science Foundation of China [Grant No.82350002], Zhongda Hospital Affiliated to Southeast University, Jiangsu Province High-Level Hospital Construction Funds [CZXM-GSP-KY].

Disclosure

All authors declare that the research was conducted in the absence of any commercial or financial relationships that could be construed as a potential conflict of interest.

References

1. Kakulas BA. A review of the neuropathology of human spinal cord injury with emphasis on special features. *J Spinal Cord Med*. 1999;22(2):119–124. doi:10.1080/10790268.1999.11719557
2. Petersen JA, Wilm BJ, von Meyenburg J, et al. Chronic cervical spinal cord injury: DTI correlates with clinical and electrophysiological measures. *J Neurotrauma*. 2012;29(8):1556–1566. doi:10.1089/neu.2011.2027
3. Barthelemy D, Willerslev-Olsen M, Lundell H, Biering-Sorensen F, Nielsen JB. Assessment of transmission in specific descending pathways in relation to gait and balance following spinal cord injury. *Prog Brain Res*. 2015;218:79–101.
4. Sangari S, Lundell H, Kirshblum S, Perez MA. Residual descending motor pathways influence spasticity after spinal cord injury. *Ann Neurol*. 2019;86(1):28–41. doi:10.1002/ana.25505
5. Asboth L, Friedli L, Beauparlant J, et al. Cortico-reticulo-spinal circuit reorganization enables functional recovery after severe spinal cord contusion. *Nat Neurosci*. 2018;21(4):576–588. doi:10.1038/s41593-018-0093-5
6. Engmann AK, Bizzozzero F, Schneider MP, et al. The gigantocellular reticular nucleus plays a significant role in locomotor recovery after incomplete spinal cord injury. *J Neurosci*. 2020;40(43):8292–8305. doi:10.1523/JNEUROSCI.0474-20.2020
7. Garcia-Rill E, Skinner RD. The mesencephalic locomotor region. II. Projections to reticulospinal neurons. *Brain Res*. 1987;411(1):13–20. doi:10.1016/0006-8993(87)90676-7
8. Brocard F, Dubuc R. Differential contribution of reticulospinal cells to the control of locomotion induced by the mesencephalic locomotor region. *J Neurophysiol*. 2003;90(3):1714–1727. doi:10.1152/jn.00202.2003
9. Capelli P, Pivetta C, Soledad Esposito M, Arber S. Locomotor speed control circuits in the caudal brainstem. *Nature*. 2017;551(7680):373–377. doi:10.1038/nature24064
10. Lemieux M, Bretzner F, Perreault M-C. Glutamatergic neurons of the gigantocellular reticular nucleus shape locomotor pattern and rhythm in the freely behaving mouse. *PLoS Biol*. 2019;17(4):e2003880. doi:10.1371/journal.pbio.2003880
11. Hagglund M, Borgius L, Dougherty KJ, Kiehn O. Activation of groups of excitatory neurons in the mammalian spinal cord or hindbrain evokes locomotion. *Nat Neurosci*. 2010;13(2):246–252. doi:10.1038/nn.2482
12. Filli L, Engmann AK, Zorner B, et al. Bridging the gap: a reticulo-propriospinal detour bypassing an incomplete spinal cord injury. *J Neurosci*. 2014;34(40):13399–13410. doi:10.1523/JNEUROSCI.0701-14.2014
13. Baker SN, Perez MA. Reticulospinal contributions to gross hand function after human spinal cord injury. *J Neurosci*. 2017;37(40):9778–9784. doi:10.1523/JNEUROSCI.3368-16.2017
14. Zaaimi B, Edgley SA, Soteropoulos DS, Baker SN. Changes in descending motor pathway connectivity after corticospinal tract lesion in macaque monkey. *Brain*. 2012;135(Pt 7):2277–2289. doi:10.1093/brain/aws115
15. Kathe C, Skinnider MA, Hutson TH, et al. The neurons that restore walking after paralysis. *Nature*. 2022;611(7936):540–547. doi:10.1038/s41586-022-05385-7
16. van den Brand R, Heutschi J, Barraud Q, et al. Restoring voluntary control of locomotion after paralyzing spinal cord injury. *Science*. 2012;336(6085):1182–1185. doi:10.1126/science.1217416
17. Barbeau H, Ladouceur M, Mirbagheri MM, Kearney RE. The effect of locomotor training combined with functional electrical stimulation in chronic spinal cord injured subjects: walking and reflex studies. *Brain Res Brain Res Rev*. 2002;40(1–3):274–291. doi:10.1016/S0165-0173(02)00210-2
18. James ND, Bartus K, Grist J, Bennett DL, McMahon SB, Bradbury EJ. Conduction failure following spinal cord injury: functional and anatomical changes from acute to chronic stages. *J Neurosci*. 2011;31(50):18543–18555. doi:10.1523/JNEUROSCI.4306-11.2011
19. Lu QB, Sun JF, Yang QY, et al. Magnetic brain stimulation using iron oxide nanoparticle-mediated selective treatment of the left prelimbic cortex as a novel strategy to rapidly improve depressive-like symptoms in mice. *Zool Res*. 2020;41(4):381–394. doi:10.24272/j.issn.2095-8137.2020.076

20. Deng ZD, Peterchev AV, Lisanby SH. Coil design considerations for deep-brain transcranial magnetic stimulation (dTMS). Annual International Conference of the IEEE Engineering in Medicine and Biology Society IEEE Engineering in Medicine and Biology Society Annual International Conference; 2008:5675–5679.
21. Lu M, Cohen MH, Rieves D, Pazdur R. FDA report: ferumoxytol for intravenous iron therapy in adult patients with chronic kidney disease. *Am J Hematol*. 2010;85(5):315–319. doi:10.1002/ajh.21656
22. Umarao P, Bose S, Bhattacharyya S, Kumar A, Jain S. Neuroprotective potential of superparamagnetic iron oxide nanoparticles along with exposure to electromagnetic field in 6-OHDA rat model of Parkinson's disease. *J Nanosci Nanotechnol*. 2016;16(1):261–269. doi:10.1166/jnn.2016.11103
23. Pal A, Singh A, Nag TC, Chattopadhyay P, Mathur R, Jain S. Iron oxide nanoparticles and magnetic field exposure promote functional recovery by attenuating free radical-induced damage in rats with spinal cord transection. *Int J Nanomed*. 2013;8:2259–2272. doi:10.2147/IJN.S44238
24. Hicks AL. Locomotor training in people with spinal cord injury: is this exercise? *Spinal Cord*. 2021;59(1):9–16. doi:10.1038/s41393-020-0502-y
25. Sun T, Ye C, Wu J, Zhang Z, Cai Y, Yue F. Treadmill step training promotes spinal cord neural plasticity after incomplete spinal cord injury. *Neural Regen Res*. 2013;8(27):2540–2547. doi:10.3969/j.issn.1673-5374.2013.27.005
26. Wang H, Liu NK, Zhang YP, et al. Treadmill training induced lumbar motoneuron dendritic plasticity and behavior recovery in adult rats after a thoracic contusive spinal cord injury. *Exp Neurol*. 2015;271:368–378. doi:10.1016/j.expneurol.2015.07.004
27. Wu M, Kim J, Wei F. Facilitating weight shifting during treadmill training improves walking function in humans with spinal cord injury: a randomized controlled pilot study. *Ame J Phys Med Rehabilitat*. 2018;97(8):585–592. doi:10.1097/PHM.0000000000000927
28. Wagner FB, Mignardot JB, Le goff-mignardot CG, et al. Targeted neurotechnology restores walking in humans with spinal cord injury. *Nature*. 2018;563(7729):65–71. doi:10.1038/s41586-018-0649-2
29. Bonizzato M, James ND, Pidpruzhnykova G, et al. Multi-pronged neuromodulation intervention engages the residual motor circuitry to facilitate walking in a rat model of spinal cord injury. *Nat Commun*. 2021;12(1):1925. doi:10.1038/s41467-021-22137-9
30. Wang P, Yin R, Wang S, et al. Effects of Repetitive Transcranial Magnetic Stimulation (rTMS) and treadmill training on recovery of motor function in a rat model of partial spinal cord injury. *Med Sci Monit*. 2021;27:e931601. doi:10.12659/MSM.931601
31. Wang S, Wang P, Yin R, et al. Combination of repetitive transcranial magnetic stimulation and treadmill training reduces hyperreflexia by rebalancing motoneuron excitability in rats after spinal cord contusion. *Neurosci Lett*. 2022;775:136536. doi:10.1016/j.neulet.2022.136536
32. Wu X, Qu W, Bakare AA, et al. A laser-guided spinal cord displacement injury in adult mice. *J Neurotrauma*. 2019;36(3):460–468. doi:10.1089/neu.2018.5756
33. Basso DM, Fisher LC, Anderson AJ, Jakeman LB, McTigue DM, Popovich PG. Basso Mouse Scale for locomotion detects differences in recovery after spinal cord injury in five common mouse strains. *J Neurotrauma*. 2006;23(5):635–659. doi:10.1089/neu.2006.23.635
34. Orlando C, Raineteau O. Integrity of cortical perineuronal nets influences corticospinal tract plasticity after spinal cord injury. *Brain Struct Funct*. 2015;220(2):1077–1091. doi:10.1007/s00429-013-0701-9
35. Yang J, Liang R, Wang L, Zheng C, Xiao X, Ming D. Repetitive Transcranial Magnetic Stimulation (rTMS) improves the gait disorders of rats under simulated microgravity conditions associated with the regulation of motor cortex. *Front Physiol*. 2021;12:587515. doi:10.3389/fphys.2021.587515
36. Redondo-Castro E, Navarro X, García-Alías G. Longitudinal evaluation of residual cortical and subcortical motor evoked potentials in spinal cord injured rats. *J Neurotrauma*. 2016;33(10):907–916. doi:10.1089/neu.2015.4140
37. Su L, Zhang B, Huang Y, Zhang H, Xu Q, Tan J. Superparamagnetic iron oxide nanoparticles modified with dimyristoylphosphatidylcholine and their distribution in the brain after injection in the rat substantia nigra. *Mater Sci Eng C Mater Biol Appl*. 2017;81:400–406. doi:10.1016/j.msec.2017.08.049
38. Liang H, Watson C, Paxinos G. Terminations of reticulospinal fibers originating from the gigantocellular reticular formation in the mouse spinal cord. *Brain Struct Funct*. 2016;221(3):1623–1633. doi:10.1007/s00429-015-0993-z
39. Chao OY, Pum ME, Li JS, Huston JP. The grid-walking test: assessment of sensorimotor deficits after moderate or severe dopamine depletion by 6-hydroxydopamine lesions in the dorsal striatum and medial forebrain bundle. *Neuroscience*. 2012;202:318–325. doi:10.1016/j.neuroscience.2011.11.016
40. Bachmann LC, Matis A, Lindau NT, Felder P, Gullo M, Schwab ME. Deep brain stimulation of the midbrain locomotor region improves paretic hindlimb function after spinal cord injury in rats. *Sci Trans Med*. 2013;5(208). doi:10.1126/scitranslmed.3005972
41. Jo HJ, Perez MA. Corticospinal-motor neuronal plasticity promotes exercise-mediated recovery in humans with spinal cord injury. *Brain*. 2020;143(5):1368–1382. doi:10.1093/brain/awaa052
42. Zhang J, Zhang D, McQuade JS, Behbehani M, Tsien JZ, Xu M. c-fos regulates neuronal excitability and survival. *Nature Genet*. 2002;30(4):416–420. doi:10.1038/ng859
43. Tillakaratne NJ, de Leon RD, Hoang TX, Roy RR, Edgerton VR, Tobin AJ. Use-dependent modulation of inhibitory capacity in the feline lumbar spinal cord. *J Neurosci*. 2002;22(8):3130–3143. doi:10.1523/JNEUROSCI.22-08-03130.2002
44. Bertels H, Vicente-Ortiz G, El Kanbi K, Takeoka A. Neurotransmitter phenotype switching by spinal excitatory interneurons regulates locomotor recovery after spinal cord injury. *Nat Neurosci*. 2022;25(5):617–629. doi:10.1038/s41593-022-01067-9
45. Tillakaratne NJ, Mouria M, Ziv NB, Roy RR, Edgerton VR, Tobin AJ. Increased expression of glutamate decarboxylase (GAD(67)) in feline lumbar spinal cord after complete thoracic spinal cord transection. *J Neurosci Res*. 2000;60(2):219–230. doi:10.1002/(SICI)1097-4547(20000415)60:2<219::AID-JNR11>3.0.CO;2-F
46. Martin EM, Devidze N, Shelley DN, Westberg L, Fontaine C, Pfaff DW. Molecular and neuroanatomical characterization of single neurons in the mouse medullary gigantocellular reticular nucleus. *J Comp Neurol*. 2011;519(13):2574–2593. doi:10.1002/cne.22639
47. Juvin L, Gratsch S, Trillaud-Doppia E, Gariepy JF, Buschges A, Dubuc R. A Specific Population of Reticulospinal Neurons Controls the Termination of Locomotion. *Cell Rep*. 2016;15(11):2377–2386. doi:10.1016/j.celrep.2016.05.029
48. Takakusaki K, Chiba R, Nozu T, Okumura T. Brainstem control of locomotion and muscle tone with special reference to the role of the mesopontine tegmentum and medullary reticulospinal systems. *J Neural Transm*. 2016;123(7):695–729. doi:10.1007/s00702-015-1475-4
49. Sangari S, Perez MA. Distinct corticospinal and reticulospinal contributions to voluntary control of elbow flexor and extensor muscles in humans with tetraplegia. *J Neurosci*. 2020;40(46):8831–8841. doi:10.1523/JNEUROSCI.1107-20.2020

50. Roussel M, Lafrance-Zoubga D, Josset N, Lemieux M, Bretzner F. Functional contribution of mesencephalic locomotor region nuclei to locomotor recovery after spinal cord injury. *Cell Rep Med*. 2023;4(2):100946. doi:10.1016/j.xcrm.2023.100946
51. Stieglitz LH, Hofer AS, Bolliger M, et al. Deep brain stimulation for locomotion in incomplete human spinal cord injury (DBS-SCI): protocol of a prospective one-armed multi-centre study. *BMJ open*. 2021;11(9):e047670. doi:10.1136/bmjopen-2020-047670
52. Kondiles BR, Murphy RL, Widman AJ, Perlmutter SI, Horner PJ. Cortical stimulation leads to shortened myelin sheaths and increased axonal branching in spared axons after cervical spinal cord injury. *Glia*. 2023;71(8):1947–1959. doi:10.1002/glia.24376
53. Korzhova J, Sinitsyn D, Chervyakov A, et al. Transcranial and spinal cord magnetic stimulation in treatment of spasticity: a literature review and meta-analysis. *Eur J Phys Rehabil Med*. 2018;54(1):75–84. doi:10.23736/S1973-9087.16.04433-6
54. Shefchyk SJ, Jell RM, Jordan LM. Reversible cooling of the brainstem reveals areas required for mesencephalic locomotor region evoked treadmill locomotion. *Exp Brain Res*. 1984;56(2):257–262. doi:10.1007/BF00236281
55. Kim LH, Sharma S, Sharples SA, Mayr KA, Kwok CHT, Whelan PJ. Integration of descending command systems for the generation of context-specific locomotor behaviors. *Front Neurosci*. 2017;11:581. doi:10.3389/fnins.2017.00581
56. Reis DJ, Granata AR, Joh TH, Ross CA, Ruggiero DA, Park DH. Brain stem catecholamine mechanisms in tonic and reflex control of blood pressure. *Hypertension*. 1984;6(5 Pt 2):Ii7–Ii15. doi:10.1161/01.HYP.6.5_Pt_2.II7
57. Lee HJ, Jakovcevski I, Radonjic N, Hoelters L, Schachner M, Irintchev A. Better functional outcome of compression spinal cord injury in mice is associated with enhanced H-reflex responses. *Exp Neurol*. 2009;216(2):365–374. doi:10.1016/j.expneurol.2008.12.009
58. Hofer AS, Scheuber MI, Sartori AM, et al. Stimulation of the cuneiform nucleus enables training and boosts recovery after spinal cord injury. *Brain*. 2022;145(10):3681–3697. doi:10.1093/brain/awac184
59. Chaudhry FA, Reimer RJ, Bellocchio EE, et al. The vesicular GABA transporter, VGAT, localizes to synaptic vesicles in sets of glycinergic as well as GABAergic neurons. *J Neurosci*. 1998;18(23):9733–9750. doi:10.1523/JNEUROSCI.18-23-09733.1998
60. Yao X. The role of GABA in spinal cord injury. *Neurospine*. 2022;19(3):669–670. doi:10.14245/ns.2244666.333
61. de Sousa N, Santos D, Monteiro S, Silva N, Barreiro-Iglesias A, Salgado AJ. Role of baclofen in modulating spasticity and neuroprotection in spinal cord injury. *J Neurotrauma*. 2022;39(3–4):249–258. doi:10.1089/neu.2020.7591
62. Cao Y, Wilcox KS, Martin CE, Rachinsky TL, Eberwine J, Dichter MA. Presence of mRNA for glutamic acid decarboxylase in both excitatory and inhibitory neurons. *Proc Natl Acad Sci U S A*. 1996;93(18):9844–9849. doi:10.1073/pnas.93.18.9844
63. Kitzman P. Changes in vesicular glutamate transporter 2, vesicular GABA transporter and vesicular acetylcholine transporter labeling of sacrocaudal motoneurons in the spastic rat. *Exp Neurol*. 2006;197(2):407–419. doi:10.1016/j.expneurol.2005.10.005
64. Robinson GA, Goldberger ME. Interfering with inhibition may improve motor function. *Brain Res*. 1985;346(2):400–403. doi:10.1016/0006-8993(85)90879-0
65. Dolbow DR, Davis GM, Welsch M, Gorgey AS. Benefits and interval training in individuals with spinal cord injury: a thematic review. *J Spinal Cord Med*. 2022;45(3):327–338. doi:10.1080/10790268.2021.2002020
66. Battistuzzo CR, Rank MM, Flynn JR, et al. Gait recovery following spinal cord injury in mice: limited effect of treadmill training. *J Spinal Cord Med*. 2016;39(3):335–343. doi:10.1080/10790268.2015.1133017
67. Wolpaw JR. Treadmill training after spinal cord injury: good but not better. *Neurology*. 2006;66(4):466–467. doi:10.1212/01.wnl.0000203915.14930.b4
68. Duan R, Qu M, Yuan Y, et al. Clinical benefit of rehabilitation training in spinal cord injury: a systematic review and meta-analysis. *Spine*. 2021;46(6):E398–E410. doi:10.1097/BRS.0000000000003789
69. Courtine G, Gerasimenko Y, van den Brand R, et al. Transformation of nonfunctional spinal circuits into functional states after the loss of brain input. *Nat Neurosci*. 2009;12(10):1333–1342. doi:10.1038/nn.2401